# Hall and Nernst Coefficients of Underdoped $HgBa_2CuO_{4+\delta}$ : Fermi-Surface Reconstruction in an Archetypal Cuprate Superconductor

Nicolas Doiron-Leyraud,[1,*] S. Lepault,[2] O. Cyr-Choinière,[1] B. Vignolle,[2] F. Laliberté,[1] J. Chang,[1] N. Barišić,[3] M. K. Chan,[3] L. Ji,[3] X. Zhao,[3,4] Y. Li,[5] M. Greven,[3] C. Proust,[2,6] and Louis Taillefer[1,6,†]

[1] *Département de physique & RQMP, Université de Sherbrooke, Sherbrooke, Québec, Canada J1K 2R1*
[2] *Laboratoire National des Champs Magnétiques Intenses, UPR 3228, (CNRS-INSA-UJF-UPS), Toulouse 31400, France*
[3] *School of Physics and Astronomy, University of Minnesota, Minneapolis, Minnesota 55455, USA*
[4] *State Key Lab of Inorganic Synthesis and Preparative Chemistry, College of Chemistry, Jilin University, Changchun 130012, China*
[5] *International Center for Quantum Materials, School of Physics, Peking University, Beijing 100871, China*
[6] *Canadian Institute for Advanced Research, Toronto, Ontario, Canada M5G 1Z8*

(Dated: November 1, 2012)

The Hall coefficient $R_{\rm H}$ of underdoped $HgBa_2CuO_{4+\delta}$ (Hg1201) was measured at low temperature in magnetic fields large enough to suppress superconductivity. The normal-state $R_{\rm H}(T)$ is found to drop with decreasing temperature and become negative below 10 K, as also observed in the orthorhombic bi-layer cuprate $YBa_2Cu_3O_y$ (YBCO) at comparable doping. In YBCO, the negative $R_{\rm H}$ is the signature of a Fermi-surface reconstruction that produces a small electron pocket, attributed to the onset of charge-density wave order at low temperature. We infer that a similar Fermi-surface reconstruction occurs in the tetragonal single-layer material Hg1201. A striking similarity is also found in the normal-state Nernst coefficient $\nu(T)$, which drops below the pseudogap temperature $T^\star$, to reach a large negative value at low temperature, in both Hg1201 and YBCO. Our results are compelling evidence that the mechanisms responsible for Fermi-surface reconstruction and pseudogap formation in hole-doped cuprates are universal.

Understanding the phase diagram of cuprates is a central challenge of high-temperature superconductivity. In the $La_2CuO_4$ family of cuprates, where the maximal superconducting critical temperature $T_c$ does not exceed 40 K, the existence of density-wave order involving spin and charge modulations, known as stripe order [1, 2], has been established over a wide range of hole dopings $p$ [3, 4]. Until recently, however, no evidence of density-wave order had been reported for a cuprate with a high maximal $T_c$, except at very low doping [5]. In YBCO, whose maximal $T_c$ is 94 K, hints of density-wave order first came from the observation of a small electron pocket [6], as detected in quantum oscillations [7] and Hall effect measurements [8]. The likely mechanism for the formation of a small electron pocket is a Fermi surface reconstruction (FSR) by some density-wave modulation that breaks the translational symmetry of the lattice [9], as seen for example in electron-doped cuprates [10–12]. Thermoelectric measurements on YBCO and $La_{1.8-x}Eu_{0.2}Sr_xCuO_4$ (Eu-LSCO) revealed a detailed similarity between the two materials as a function of temperature and doping [13, 14], with negative Seebeck coefficient at low temperature, indicating that FSR by stripe order is at play in both. This was confirmed when charge-stripe order was detected in YBCO via high-field nuclear magnetic resonance (NMR) measurements [15], precisely in the range of temperature and doping where $R_{\rm H}$ is negative [16]. The question of whether charge-density-wave order is the generic non-superconducting ground state of underdoped cuprates is vital since it raises the possibility that it might play a fundamental role in the pairing mechanism and in the anomalous scattering [17, 18] that causes the linear-$T$ resistivity [19, 20]. To answer that question we need to examine a cuprate material with a high maximal $T_c$ and none of the structural peculiarities of YBCO – with its unidirectional CuO chains that make it orthorhombic – or Eu-LSCO – with its low-temperature tetragonal (LTT) structure favorable to stripe order. Hg1201, a single-layer tetragonal cuprate with the highest maximal $T_c$ of all single-layer cuprates (97 K), is one such model material [21, 22]. In this Letter, we present measurements of the Hall and Nernst coefficients in underdoped Hg1201 that reveal a FSR very similar to that of YBCO. This is compelling evidence that density-wave modulations are an intrinsic tendency of a hole-doped $CuO_2$ plane.

*Methods.* – The Hall coefficient $R_{\rm H} \equiv \rho_{xy}/H$ was measured in two nominally identical high-purity single crystals of underdoped Hg1201 with $T_c \simeq 65$ K (samples A and B), prepared as described elsewhere [21, 22]. According to the $T_c(p)$ relationship for Hg1201 established in ref. 23, our samples have a doping $p \simeq 0.075$. Measurements were performed in pulsed magnetic fields at the LNCMI in Toulouse, as described previously [8]. The maximum field was $H = 59$ T and 68 T for sample A and B, respectively. The Nernst coefficient $\nu \equiv N/H$ was measured on sample A at Sherbrooke in a field of $H = 10$ T, as described previously [24].

*Hall effect and FSR.* – In Fig. 1a, the Hall coefficient $R_{\rm H}$ is plotted as a function of magnetic field $H$ up to 70 T, for different temperatures down to $T = 4.2$ K. All isotherms of sample A (B) saturate at high fields, beyond $H = 53$ T (68 T), except (including) at $T = 4.2$ K. In

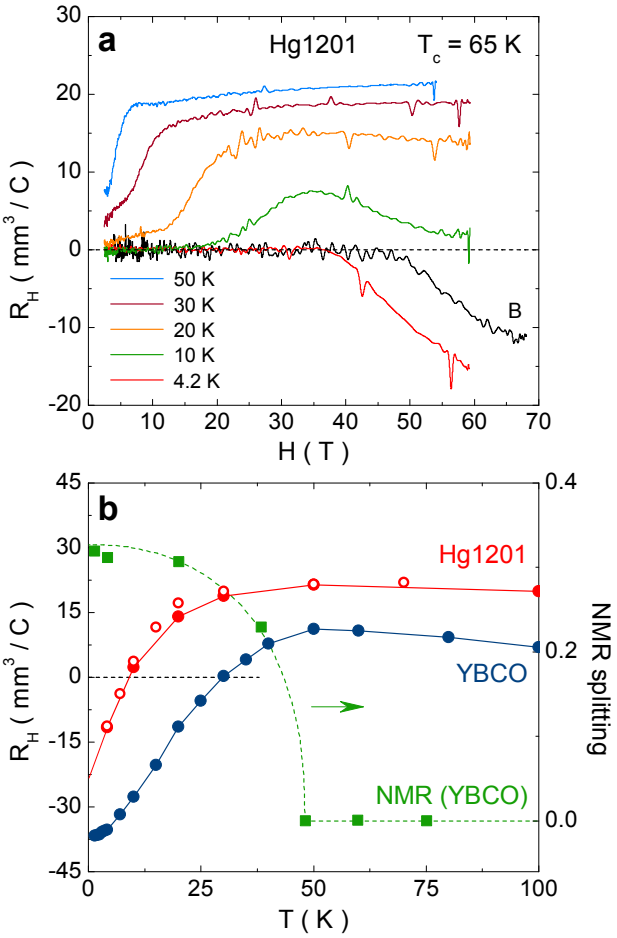


FIG. 1. a) Hall coefficient $R_{\rm H}$ of Hg1201 as a function of magnetic field $H$, in sample A at various temperatures, as indicated. Also shown is an isotherm at $T = 4.2$ K measured on sample B (black curve, labelled B). b) Normal-state Hall coefficient $R_{\rm H}$ as a function of temperature, at $H = 53$ T (sample A; closed red circles, left axis) and $H = 68$ T (sample B; open red circles, left axis). Corresponding data are shown for YBCO at $p = 0.10$ and $H = 55$ T (blue circles, left axis; from [8]). Note how in both materials $R_{\rm H}(T)$ drops at low temperature to become negative, the signature of FSR [6]. We reproduce the splitting of NMR lines in YBCO at $p = 0.10$ and $H = 28.5$ T, which reveals the onset of charge order below $T_{\rm CO} \simeq 50$ K (green squares, right axis; from [15]).

Fig. 1b, the high-field normal-state value of $R_{\rm H}$ is plotted versus temperature. As expected for a hole-doped material, $R_{\rm H}$ is positive at high temperature. However, with decreasing temperature $R_{\rm H}(T)$ starts to fall below $T \simeq 50$ K to eventually become negative below the sign-change temperature $T_0 = 10 \pm 1$ K. This is our central finding: the low-temperature normal state of Hg1201 has a negative Hall coefficient.

In Fig. 1b, comparison with corresponding data in underdoped YBCO, with $T_c \simeq 57$ K ($p = 0.1$) [8], reveals a striking similarity between the two cuprates. In YBCO,

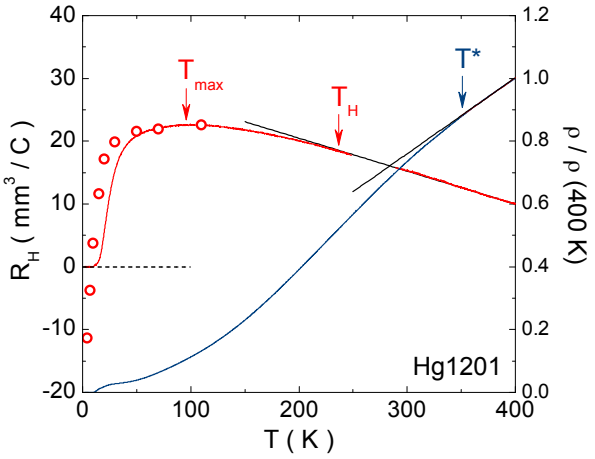


FIG. 2. In-plane electrical resistivity $\rho$ ($H = 16$ T; blue) and Hall coefficient $R_{\rm H}$ ($H = 16$ T; red) of Hg1201 measured in sample B as a function of temperature. Also shown is $R_{\rm H}$ at $H = 68$ T (open red circles). Arrows mark the characteristic temperatures $T_{\rm max} = 100 \pm 10$ K, $T_{\rm H} = 240 \pm 20$ K and $T^\star = 350 \pm 20$ K (see text). $\rho$ is field-independent at high temperature and so is $T^\star$.

there is compelling evidence that the negative $R_{\rm H}$ comes from the presence of a small electron pocket in the Fermi surface at low temperature. This evidence includes quantum oscillations [7, 25] with a frequency $F$ and mass $m^\star$ that account precisely for the residual linear term in the normal-state Seebeck coefficient $S$ at $T \to 0$, whereby $S/T \propto m^\star/F$, given that $S/T$ is negative [13, 14]. We deduce that the Fermi surface of underdoped Hg1201 at low temperature also contains an electron pocket.

This implies that the Fermi surface of Hg1201 has undergone a reconstruction, relative to its topology at high doping, where it is expected to be a single large hole-like cylinder, as in the case of the single-layer tetragonal cuprate $Tl_2Ba_2CuO_{6+\delta}$ at $p \simeq 0.25$ [26–28]. Therefore, as the doping is reduced from $p \simeq 0.25$, there will be a critical point where the Fermi surface of Hg1201 undergoes a transformation that produces an electron pocket.

Our Hall data show that a transformation also occurs upon cooling at fixed $p$, albeit smoothly, with no sign of a sharp transition. The onset of FSR may be defined as the temperature $T_{\rm max}$ below which $R_{\rm H}(T)$ starts to drop, although $R_{\rm H}(T)$ clearly starts to deviate downward from its high-temperature behavior well above $T_{\rm max}$, at a temperature labeled $T_{\rm H}$. In Fig. 2, Hall data on Hg1201 sample B yield $T_{\rm max} \simeq 100$ K and $T_{\rm H} \simeq 240$ K. In YBCO, $T_{\rm max} \simeq 100$ K and $T_{\rm H} \simeq 120$ K at $p = 0.12$ [16]. In Fig. 3, the temperatures $T_0$, $T_{\rm max}$ and $T_{\rm H}$ in YBCO and Hg1201 are plotted on their respective phase diagrams.

In YBCO, a static modulation of the charge density was detected in the $CuO_2$ planes by NMR measurements at high fields, at dopings $p = 0.10$ and 0.12 [15]. It was inferred to be unidirectional, with a period of $4a_0$

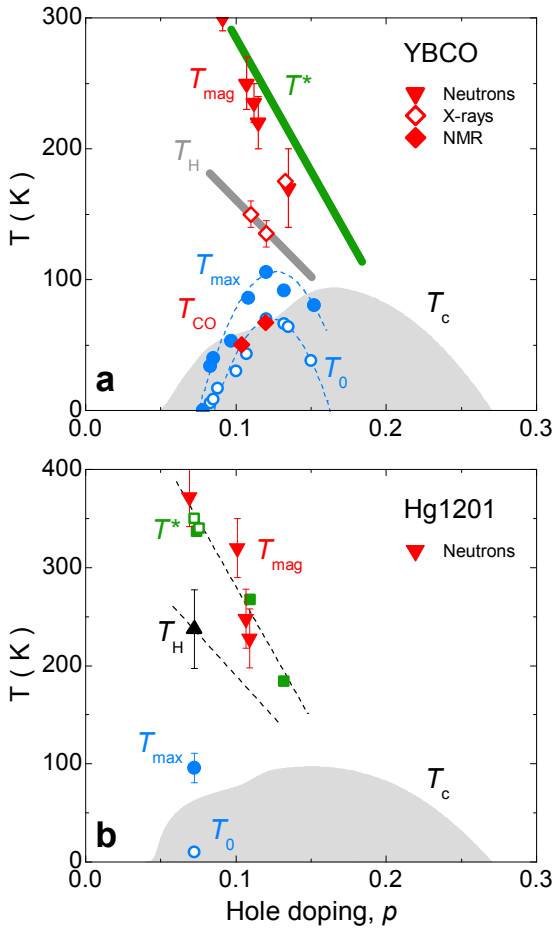


FIG. 3. a) Temperature-doping phase diagram of YBCO, showing the zero-field superconducting phase below $T_c$ (grey dome, from [29]) and the onset of $q = 0$ magnetic order below $T_{\rm mag}$ detected by spin-polarized neutron scattering (down triangles, from [30]). Several characteristic temperatures of the transport properties are displayed: the thick green and grey lines schematically represent the pseudogap temperature $T^\star$, from resistivity and Nernst data [24], and $T_{\rm H}$, from $R_{\rm H}(T)$ [16], respectively. $T_{\rm max}$ (full circles) and $T_0$ (empty circles) are determined from $R_{\rm H}(T)$ [16] (see text). We also show the onset of charge order at $T_{\rm CO}$ via NMR (full diamonds, from [15]) and the approximate onset of charge modulations via X-ray scattering (open diamonds, from [31–33]). b) Corresponding phase diagram for Hg1201, showing $T_c$ (grey dome, from [23]), $T_{\rm mag}$ (down triangles, from [34, 35]) and $T^\star$ from resistivity (full squares, from [22, 34, 35]; open squares, from this work). The characteristic temperatures of $R_{\rm H}(T)$ come from Figs. 1 and 2. All dashed lines in both panels are a guide to the eye.

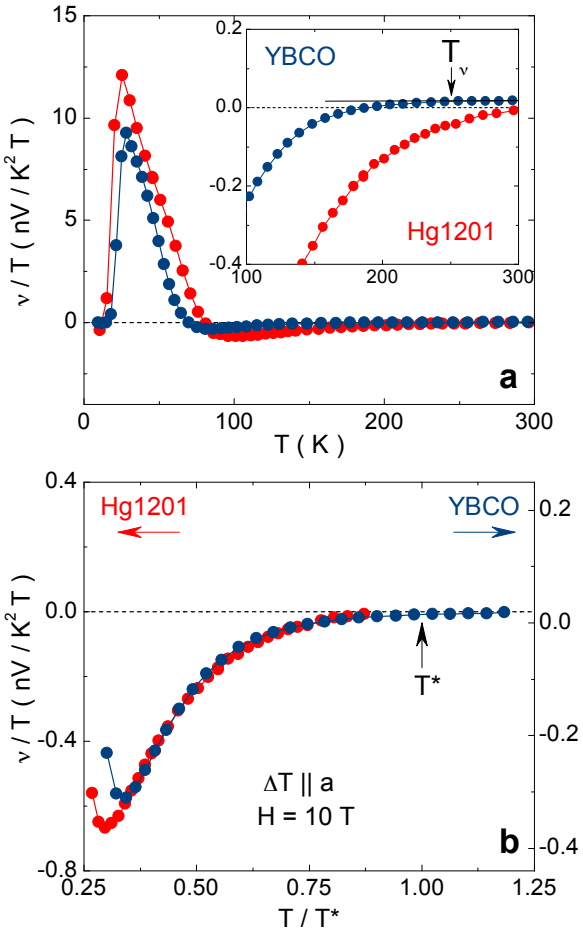


FIG. 4. a) Nernst coefficient $\nu$ of Hg1201 ($T_c = 65$ K; red, sample A) and YBCO ($T_c = 66$ K, $p = 0.12$; blue, from [24]), plotted as $\nu/T$ vs $T$. The magnetic field $H = 10$ T is along the $c$ axis and the heat gradient is along the $a$ axis. The large positive peak below $T \simeq 80$ K is due to superconductivity [36]. *Inset*: Zoom at high temperature. The blue arrow at $T_\nu = 250 \pm 20$ K marks the temperature below which $\nu/T$ in YBCO starts to fall from its small constant value at high temperature [24]. b) Same data plotted as $\nu/T$ vs $T/T^\star$, with $T^\star = 340$ K for Hg1201 and $T^\star = 250$ K for YBCO. (Note the different vertical scales for Hg1201 (red, left axis) and YBCO (blue, right axis).) Below $T/T^\star = 1.0$, the quasiparticle signal falls gradually to reach large negative values, in identical fashion in the two materials.

along the $a$ axis of the orthorhombic lattice for the ortho-II structure (the pattern could not be determined for ortho-VIII by NMR). In Fig. 1b, we reproduce the NMR data at $p = 0.11$ and see that the onset of charge order, at $T_{\rm CO} = 50 \pm 10$ K, coincides with the downturn in $R_{\rm H}(T)$ for a similar doping ($p = 0.10$). Moreover, an increase in doping to $p = 0.12$ causes a parallel increase in both $T_{\rm CO}$ [15] and $T_{\rm max}$ [16] (see Fig. 3a). This is strong evidence that the FSR in YBCO is caused by this charge order [37].

In Eu-LSCO, unidirectional stripe-like charge order with a period $4a_0$ was detected by X-ray scattering [38], with $T_{\rm CO} \simeq 40$ K at $p = 0.10$ and $T_{\rm CO} \simeq 80$ K at $p = 0.12$ [4], and linked to a drop in $R_{\rm H}(T)$ [6, 39], again showing that charge order is causing the FSR. The normal-state Seebeck coefficient in both Eu-LSCO and YBCO changes sign upon cooling [14], being negative at $T \to 0$ over the same doping range, from $p = 0.08$ to

$p \simeq 0.17$. This further shows that a similar mechanism of FSR takes place in the two materials. The evidence for FSR in Hg1201, a material whose structure has no unidirectional character, shows that density-wave order is a generic tendency of the square $CuO_2$ plane. It is therefore a fundamental phenomenon, intrinsic to the physics of cuprates. Of course, the nature of the density-wave order responsible for FSR in Hg1201 remains to be elucidated, *e.g.* by X-ray scattering or NMR studies. However, by analogy with YBCO and Eu-LSCO, it is very likely to involve charge modulations, but perhaps not unidirectional. Recent X-ray studies of YBCO have discovered charge modulations (which may not be static) in both in-plane directions (along $a$ and $b$ axes), with a period closer to $3a_0$ [31–33]. Present in zero magnetic field, they emerge at temperatures close to $T_{\rm H}$ (Fig. 3). Their relation to the static field-induced charge order seen by NMR below $T_{\rm CO}$ remains to be understood. Prior to this, it was proposed that a bidirectional charge order could be part of the explanation for the reconstructed Fermi surface of underdoped YBCO [40].

Certain features of the lattice structure may play a role in stabilizing the charge order, strengthening it more in some materials (*e.g.* with the LTT structure). This would impact on the competition between charge order and superconductivity, suppressing $T_c$ more effectively in Eu-LSCO (maximal $T_c \simeq 20$ K), where charge order exists at $H = 0$, than in YBCO (where a magnetic field is needed to induce charge order) or in Hg1201 (maximal $T_c = 97$ K). Note that in YBCO [29], $T_c$ is suppressed in the region of the phase diagram where the electron pocket exists [16]. A similar $T_c$ suppression in the underdoped region is seen in Hg1201 [23].

*Nernst effect and pseudogap phase.* – In underdoped YBCO, downturns due to FSR are not only seen in $R_{\rm H}(T)$ [8, 16] and $S/T$ [13, 14], but also in the Nernst coefficient $\nu(T)$ [13, 24]. In Fig. 4, the Nernst coefficient $\nu$ of YBCO at $p = 0.12$ is seen to deviate from its high-temperature behavior, where $\nu/T$ is small and constant, below a temperature $T_\nu \simeq 250$ K. It drops monotonically until a large positive signal due to superconductivity rises close to $T_c$ [36]. Application of a large magnetic field to suppress this signal reveals that the smooth drop in the normal-state $\nu/T$ continues monotonically down to $T = 0$ [13, 41]. The value of $|\nu/T|$ at $T \to 0$ is precisely that expected of the electron Fermi surface [14], given its frequency, mass and mobility measured via quantum oscillations [7, 25]. Therefore, the change in the electronic properties that eventually leads to the reconstructed Fermi surface at $T = 0$ may actually start at $T_\nu$. In YBCO, $T_\nu \simeq T^\star$ as a function of doping [24] (Fig. 3), where $T^\star$ is the pseudogap temperature at which the in-plane resistivity $\rho_a(T)$ deviates from its linear temperature dependence at high temperature.

In Fig. 4, we report the Nernst coefficient of Hg1201, seen to be essentially identical to that of YBCO. When plotted as a function of $T/T^\star$, $\nu/T$ has the exact same temperature dependence in both materials, starting from a small flat value at high temperature, dropping smoothly to reach a large negative value at low temperature. (Note that in YBCO $\nu$ is anisotropic in the $ab$ plane [24, 41]. In tetragonal Hg1201, where no such anisotropy is expected, the magnitude of $\nu$ lies between the $\nu_a$ and $\nu_b$ of YBCO.) $T^\star$ in Hg1201 is defined as in YBCO, by the temperature below which the in-plane resistivity $\rho_a(T)$ deviates from its linear-$T$ dependence at high temperature [22, 34, 35]. Resistivity data yield $T^\star = 340 \pm 20$ K and $350 \pm 20$ K in samples A and B (Fig. 2), respectively, in agreement with previous measurements [22, 34, 35]. It should be mentioned that our samples exhibit a Fermi liquid-like $T^2$ resistivity below a temperature $T^{\star\star}$, this being another common feature of Hg1201 and YBCO [42]. For our sample, $T^{\star\star} \simeq 200$ K $\simeq T_{\rm H}$, and $R_{\rm H}(T)$ is roughly constant in the range of $T^2$ resistivity.

Given the striking similarity in the various transport properties of YBCO and Hg1201, and in their phase diagrams (Fig. 3), we conclude that the same microscopic mechanisms must be involved in both and these must therefore be generic to hole-doped cuprates. FSR in YBCO is caused by charge order, which sets in below $T_{\rm CO} \simeq 70$ K at $p = 0.12$ [15]. However, signs of this reconstruction are clearly seen well above $T_{\rm CO}$ — up to $T_{\rm H} \simeq 120$ K in $R_{\rm H}(T)$ and apparently as high as $T^\star$ in $\rho(T)$ and $\nu(T)$. The combined transport properties are consistent with a scenario in which the pseudogap phase would be a high-temperature precursor of the charge-ordered phase at low temperature. Recent observations, via X-ray scattering [31–33], of charge modulations in YBCO up to $\sim$ 150 K lend support to this scenario. A precursor regime of this kind is observed in the iron-arsenide superconductor $Ba(Fe_{1-x}Co_x)_2As_2$, where signatures of FSR are detected in the resistivity at temperatures up to 2-3 times the antiferromagnetic ordering temperature [43]. Note that a $q = 0$ magnetic order, seen via polarized neutron scattering, is present below $T_{\rm mag} \simeq T^\star$ in both Hg1201 [34, 35] and YBCO [30], and polar Kerr-effect measurements have revealed evidence of a broken symmetry below $T^\star$ in YBCO [44]. A phase transition in YBCO at $T^\star$ was also detected by ultrasonic attenuation [45]. However, to date, the pseudogap excitations that have been identified in Hg1201 are strictly magnetic. The relation of these various features of the pseudogap phase to the charge modulations and FSR remains to be elucidated.

The work at Sherbrooke was supported by a Canada Research Chair, CIFAR, NSERC, CFI, and FQRNT. The work at Toulouse was supported by PF7 EuroMagNET II. The work at the University of Minnesota (crystal growth, annealing, characterization and contacting of samples) was supported by the US Department of Energy, Office of Basic Energy Sciences. J. C. was supported by the Swiss National Science Foundation.

* ndl@physique.usherbrooke.ca
† louis.taillefer@usherbrooke.ca

[1] S. A. Kivelson, I. P. Bindloss, E. Fradkin, V. Oganesyan, J. M. Tranquada, A. Kapitulnik, and C. Howald, Reviews of Modern Physics **75**, 1201 (2003).
[2] M. Vojta, Advances in Physics **58**, 699 (2009).
[3] N. Ichikawa, S. Uchida, J. M. Tranquada, T. Niemller, P. M. Gehring, S. H. Lee, and J. R. Schneider, Physical review letters **85**, 1738 (2000).
[4] J. Fink, V. Soltwisch, J. Geck, E. Schierle, E. Weschke, and B. Büchner, Physical Review B **83**, 092503 (2011).
[5] D. Haug, V. Hinkov, Y. Sidis, P. Bourges, N. B. Christensen, A. Ivanov, T. Keller, C. T. Lin, and B. Keimer, New Journal of Physics **12**, 105006 (2010).
[6] L. Taillefer, Journal of Physics: Condensed Matter **21**, 164212 (2009).
[7] N. Doiron-Leyraud, C. Proust, D. LeBoeuf, J. Levallois, J.-B. Bonnemaison, R. Liang, D. A. Bonn, W. N. Hardy, and L. Taillefer, Nature **447**, 565 (2007).
[8] D. LeBoeuf, N. Doiron-Leyraud, J. Levallois, R. Daou, J.-B. Bonnemaison, N. E. Hussey, L. Balicas, B. J. Ramshaw, R. Liang, D. A. Bonn, W. N. Hardy, S. Adachi, C. Proust, and L. Taillefer, Nature **450**, 533 (2007).
[9] S. Chakravarty, Science **319**, 735 (2008).
[10] N. P. Armitage, F. Ronning, D. H. Lu, C. Kim, A. Damascelli, K. M. Shen, D. L. Feng, H. Eisaki, Z.-X. Shen, P. K. Mang, N. Kaneko, M. Greven, Y. Onose, Y. Taguchi, and Y. Tokura, Physical Review Letters **88**, 257001 (2002).
[11] Y. Dagan, M. M. Qazilbash, C. P. Hill, V. N. Kulkarni, and R. L. Greene, Physical Review Letters **92**, 167001 (2004).
[12] J. Lin and A. J. Millis, Physical Review B **72**, 214506 (2005).
[13] J. Chang, R. Daou, C. Proust, D. LeBoeuf, N. Doiron-Leyraud, F. Laliberté, B. Pingault, B. J. Ramshaw, R. Liang, D. A. Bonn, W. N. Hardy, H. Takagi, A. B. Antunes, I. Sheikin, K. Behnia, and L. Taillefer, Physical Review Letters **104**, 057005 (2010).
[14] F. Laliberté, J. Chang, N. Doiron-Leyraud, E. Hassinger, R. Daou, M. Rondeau, B. Ramshaw, R. Liang, D. Bonn, W. Hardy, S. Pyon, T. Takayama, H. Takagi, I. Sheikin, L. Malone, C. Proust, K. Behnia, and L. Taillefer, Nature Communications **2**, 432 (2011).
[15] T. Wu, H. Mayaffre, S. Krämer, M. Horvatic, C. Berthier, W. N. Hardy, R. Liang, D. A. Bonn, and M.-H. Julien, Nature **477**, 191 (2011).
[16] D. LeBoeuf, N. Doiron-Leyraud, B. Vignolle, M. Sutherland, B. Ramshaw, J. Levallois, R. Daou, F. Laliberté, O. Cyr-Choinière, J. Chang, Y. Jo, L. Balicas, R. Liang, D. Bonn, W. Hardy, C. Proust, and L. Taillefer, Physical Review B **83**, 054506 (2011).
[17] P. Monthoux, D. Pines, and G. G. Lonzarich, Nature **450**, 1177 (2007).
[18] L. Taillefer, Annual Review of Condensed Matter Physics **1**, 51 (2010).
[19] R. Daou, N. Doiron-Leyraud, D. LeBoeuf, S. Y. Li, F. Laliberté, O. Cyr-Choinière, Y. J. Jo, L. Balicas, J.-Q. Yan, J.-S. Zhou, J. B. Goodenough, and L. Taillefer, Nature Physics **5**, 31 (2009).
[20] R. A. Cooper, Y. Wang, B. Vignolle, O. J. Lipscombe, S. M. Hayden, Y. Tanabe, T. Adachi, Y. Koike, M. Nohara, H. Takagi, C. Proust, and N. E. Hussey, Science **323**, 603 (2009).
[21] X. Zhao, G. Yu, Y.-C. Cho, G. Chabot-Couture, N. Barišić, P. Bourges, N. Kaneko, Y. Li, L. Lu, E. M. Motoyama, O. P. Vajk, and M. Greven, Advanced Materials **18**, 3243 (2006).
[22] N. Barišić, Y. Li, X. Zhao, Y.-C. Cho, G. Chabot-Couture, G. Yu, and M. Greven, Physical Review B **78**, 054518 (2008).
[23] A. Yamamoto, W.-Z. Hu, and S. Tajima, Physical Review B **63**, 024504 (2000).
[24] R. Daou, J. Chang, D. LeBoeuf, O. Cyr-Choinière, F. Laliberté, N. Doiron-Leyraud, B. J. Ramshaw, R. Liang, D. A. Bonn, W. N. Hardy, and L. Taillefer, Nature **463**, 519 (2010).
[25] C. Jaudet, D. Vignolles, A. Audouard, J. Levallois, D. LeBoeuf, N. Doiron-Leyraud, B. Vignolle, M. Nardone, A. Zitouni, R. Liang, D. A. Bonn, W. N. Hardy, L. Taillefer, and C. Proust, Physical Review Letters **100**, 187005 (2008).
[26] B. Vignolle, A. Carrington, R. A. Cooper, M. M. J. French, A. P. Mackenzie, C. Jaudet, D. Vignolles, C. Proust, and N. E. Hussey, Nature **455**, 952 (2008).
[27] M. Platé, J. D. F. Mottershead, I. S. Elfimov, D. C. Peets, R. Liang, D. A. Bonn, W. N. Hardy, S. Chiuzbaian, M. Falub, M. Shi, L. Patthey, and A. Damascelli, Physical Review Letters **95**, 077001 (2005).
[28] A. P. Mackenzie, S. R. Julian, D. C. Sinclair, and C. T. Lin, Physical Review B **53**, 5848 (1996).
[29] R. Liang, D. A. Bonn, and W. N. Hardy, Physical Review B **73**, 180505 (2006).
[30] B. Fauqué, Y. Sidis, V. Hinkov, S. Pailhs, C. T. Lin, X. Chaud, and P. Bourges, Physical Review Letters **96**, 197001 (2006).
[31] G. Ghiringhelli, M. L. Tacon, M. Minola, S. Blanco-Canosa, C. Mazzoli, N. B. Brookes, G. M. D. Luca, A. Frano, D. G. Hawthorn, F. He, T. Loew, M. M. Sala, D. C. Peets, M. Salluzzo, E. Schierle, R. Sutarto, G. A. Sawatzky, E. Weschke, B. Keimer, and L. Braicovich, Science **337**, 821 (2012).
[32] J. Chang, E. Blackburn, A. T. Holmes, N. B. Christensen, J. Larsen, J. Mesot, R. Liang, D. A. Bonn, W. N. Hardy, A. Watenphul, M. v. Zimmermann, E. M. Forgan, and S. M. Hayden, Nature Physics (2012), 10.1038/nphys2456.
[33] A. J. Achkar, R. Sutarto, X. Mao, F. He, A. Frano, S. Blanco-Canosa, M. Le Tacon, G. Ghiringhelli, L. Braicovich, M. Minola, M. Moretti Sala, C. Mazzoli, R. Liang, D. A. Bonn, W. N. Hardy, B. Keimer, G. A. Sawatzky, and D. G. Hawthorn, Physical Review Letters **109**, 167001 (2012).
[34] Y. Li, V. Balédent, N. Barišić, Y. Cho, B. Fauqu, Y. Sidis, G. Yu, X. Zhao, P. Bourges, and M. Greven, Nature **455**, 372 (2008).
[35] Y. Li, V. Balédent, N. Barišić, Y. C. Cho, Y. Sidis, G. Yu, X. Zhao, P. Bourges, and M. Greven, Physical Review B **84**, 224508 (2011).
[36] J. Chang, N. Doiron-Leyraud, O. Cyr-Choinière, G. Grissonnanche, F. Laliberté, E. Hassinger, J.-P. Reid, R. Daou, S. Pyon, T. Takayama, H. Takagi, and L. Taillefer, Nature Physics **8**, 751 (2012).
[37] N. Doiron-Leyraud and L. Taillefer, Physica C: Super-

conductivity **481**, 161 (2012).
[38] J. Fink, E. Schierle, E. Weschke, J. Geck, D. Hawthorn, V. Soltwisch, H. Wadati, H.-H. Wu, H. A. Drr, N. Wizent, B. Büchner, and G. A. Sawatzky, Physical Review B **79**, 100502 (2009).
[39] O. Cyr-Choinière, R. Daou, F. Laliberté, D. LeBoeuf, N. Doiron-Leyraud, J. Chang, J.-Q. Yan, J.-G. Cheng, J.-S. Zhou, J. B. Goodenough, S. Pyon, T. Takayama, H. Takagi, Y. Tanaka, and L. Taillefer, Nature **458**, 743 (2009).
[40] N. Harrison and S. E. Sebastian, Physical Review Letters **106**, 226402 (2011).
[41] J. Chang, N. Doiron-Leyraud, F. Laliberté, R. Daou, D. LeBoeuf, B. J. Ramshaw, R. Liang, D. A. Bonn, W. N. Hardy, C. Proust, I. Sheikin, K. Behnia, and L. Taillefer, Physical Review B **84**, 014507 (2011).
[42] N. Barišić, Y. Li, G. Yu, X. Zhao, M. Dressel, A. Smontara, and M. Greven, arXiv:1207.1504 (2012).
[43] J.-H. Chu, J. G. Analytis, K. D. Greve, P. L. McMahon, Z. Islam, Y. Yamamoto, and I. R. Fisher, Science **329**, 824 (2010).
[44] J. Xia, E. Schemm, G. Deutscher, S. A. Kivelson, D. A. Bonn, W. N. Hardy, R. Liang, W. Siemons, G. Koster, M. M. Fejer, and A. Kapitulnik, Physical Review Letters **100**, 127002 (2008).
[45] A. Shekhter, A. Migliori, J. B. Betts, F. F. Balakirev, R. D. McDonald, S. C. Riggs, B. J. Ramshaw, R. Liang, W. N. Hardy, and D. A. Bonn, arXiv:1208.5810 (2012).